EUROPHYSICS LETTERS 15 August 2006

Europhys. Lett., **75** (4), pp. 659–665 (2006)
DOI: 10.1209/epl/i2006-10150-5

Tension-induced pore formation and leakage in adhering vesicles

P. Lenz[1], J. M. Johnson[2,3], Y.-H. M. Chan[2] and S. G. Boxer[2]

[1] *Philipps-Universität Marburg, Fachbereich Physik - Renthof 5 D-35032 Marburg, Germany*
[2] *Department of Chemistry, Stanford University - Stanford, CA 94305, USA*
[3] *Department of Physiology and Biophysics, University of Colorado Health Sciences Center - Denver, CO 80045, USA*

received 18 February 2006; accepted in final form 27 June 2006
published online 14 July 2006

PACS. 87.16.Dg – Membranes, bilayers, and vesicles.
PACS. 68.35.Np – Adhesion.

Abstract. – The influence of inclusion-induced tension on pore formation is studied theoretically and experimentally. It is shown that fluorescently labeled lipids can enhance pore formation and induce leakage of adhering vesicles. These effects are more pronounced for smaller vesicles. The theoretical predictions are confirmed by experimental two-color fluorescent data. Finally, the influence of the pore formation dynamics on rupture processes of vesicles is analyzed yielding a new picture of the transition to bilayer disks.

Supported lipid bilayers provide an ideal system for the investigation of cellular membrane interactions [1] such as formation of the immunological synapse [2] and SNARE driven vesicle fusion in simplified environments [3]. They are also the basis for a variety of bio-sensors [4–6]. There are several methods of forming supported bilayers, including deposition by Langmuir-Blodgett techniques [7], spreading over a surface from a bulk lipid source [8], or simply by vesicle fusion to a substrate [9].

The fundamental mechanisms leading to bilayer formation via vesicle fusion are only partially understood. It is generally believed that it proceeds via the following steps: i) vesicle adhesion, ii) vesicle fusion, and iii) vesicle rupture. This picture relies strongly on the theory developed by Lipowsky and Seifert [10,11]. In [11] it has been predicted that with increasing volume (driven by vesicle-vesicle fusion events) the adsorbed vesicles become flatter and flatter until at a critical rupture radius R^*_{bd} they undergo a transition to a bilayer disk. This has been confirmed in recent experimental studies [12–14]; however, in [15] R^*_{bd} was found to be higher than theoretically expected. There are experimental indications [16] that the strength of the adhesion potential W is a critical parameter in these processes which would explain why supported bilayers only form on very few substrates, namely those with large enough W.

Fusion and rupture transitions lead to a change in the vesicle's topology and thus require (as an essential step) the formation of holes, *i.e.* pores. In this paper, we analyze the influence of inclusion-induced tension on pore formation. This work focuses on adhering vesicles with a

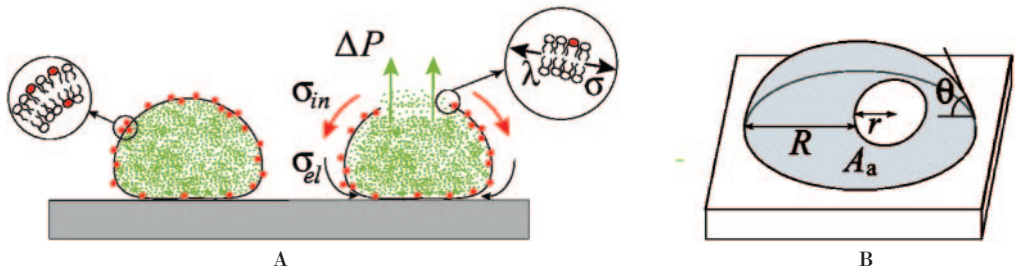

Fig. 1 – (Colour on-line) (A) Adhering vesicles with inclusions (such as fluorescent dyes, shown as red dots) are put under tension $\sigma = \sigma_{in} + \sigma_{el}$ by the adhesion potential and the interaction between inclusions. Tension causes pore formation and since there is a pressure difference ΔP between outside and inside the vesicles lose some of their encapsulated dyes (shown as green dots). As the pore expands the tension drops and the line tension λ reseals the pore. (B) For strong adhesion potential W adhering vesicles (with and without pores of radius r) adapt the shape of spherical caps with radius R, contact angle θ, and contact area $A_{\rm a}$.

particular lipid labeled with Texas Red (TR). The results however may be generally applicable to fusion of vesicles in solutions and of more complex membranes. Our model is not only a relevant extension of the Lipowsky-Seifert theory but it also yields a consistent explanation of the observations reported in [13] and [15]. To our knowledge this is the first theoretical analysis which takes into account the influence additional membrane components or inclusions have on membrane tension and thus pore formation. However, we should emphasize that we do not investigate the detailed molecular mechanisms leading to these phenomena.

The development of our model is based on the following experimental observations [13]: i) adhering TR-labeled vesicles leak. ii) This leakage is more pronounced for higher TR-concentration. iii) At the same TR-concentration no leakage occurs for vesicles in bulk. iv) Leaking vesicles appear to be much more fusogenic.

Our interpretation of these findings is that TR (which is attached to the lipid headgroup) either increases tension in the membrane or acts as a nucleation center for pores, leading in both cases to enhanced pore formation, as illustrated schematically in fig. 1A. As shown, for adhering vesicles this has the consequences that 1) smaller vesicles have a higher probability of losing their content (encapsulated dye); and 2) these vesicles are more reactive. 1) is because smaller vesicles form pores more often and the associated volume exchange with the surrounding liquid is more efficient; 2) is because smaller vesicles are better pore formers than larger ones and thus appear more fusogenic.

To derive these conclusions the dynamics of pore formation of adhering vesicles with additional inclusions has to be analyzed. The equilibrium shape of these vesicles minimizes the free energy,

$$F = \frac{1}{2}\kappa \int \mathrm{d}A\,(2H)^2 + \kappa_g \int \mathrm{d}A\,K - W A_{\rm a} + \sigma A + pV. \tag{1}$$

Here, W is the adhesion potential, κ the bending rigidity, κ_g the Gaussian rigidity, H the mean curvature, K the Gaussian curvature, σ the surface tension, $p = \Delta P$ the pressure difference between out- and inside, $A_{\rm a}$ the contact area of the vesicle, A its surface area, and V its volume. In the following an ensemble is used where σ is prescribed and A is variable. Equation (1) does not contain any contributions from the (possible) interactions between inclusions since it is assumed that they adopt an equilibrium surface concentration ρ on time scales much shorter than the lifetime of a pore [17]. But, generally, σ will depend on ρ, *i.e.* $\sigma = \sigma(\rho)$ (see

below). Finally, since fusion, rupture, and pore formation are associated with changes in the topology of the vesicles, the contribution of the Gaussian curvature is generally not negligible.

Bilayer formation occurs only for sufficiently strong adhesion potentials ($W \simeq 10^{-4}\,\mathrm{J/m^2}$). Then (up to corrections of order $\varepsilon = \sqrt{\kappa}/R\sin\theta\sqrt{W}$) adhering vesicles adapt the shape of spherical caps [18] with radius R and contact angle θ (which is determined by the area-to-volume ratio of the vesicle), cf. fig. 1B. Volume and surface area are given by $V = \pi R^3 f(\theta)/3$ and $A = \pi R^2 g(\theta)$, where $f(\theta) = 2(1-\cos\theta) - \sin^2\theta\cos\theta$ and $g(\theta) = 2(1-\cos\theta) + \sin^2\theta$.

The potential W puts the adhering vesicles under tension $\sigma_{el} = W A_\mathrm{a}/A$ [11], which leads to a stretching of the bilayer. For strong adhesion the relation between induced tension and stretching is given by [19] $\sigma_{el}(A') = \sigma_{el}(A_i) + k_a(A'-A_i)/A_i$. Here, $A'-A_i$ is the increase in the optically visible area of the vesicle with respect to the surface area of the bulk vesicle $A_i = 4\pi R_i^2$ and k_a is an "apparent tension" [20], which is related to the bare area compressibility modulus k via $k/k_a = 1 + kk_BT/(8\pi\kappa\sigma)$.

Sufficiently strong tension leads to the formation of pores. While the pore is open, tension is released, the volume of the vesicle decreases, and the pore reseals. The experimentally observed leakage is an indication that inclusions in the membrane can enhance pore formation. In particular, vesicles with TR-labeled lipids must be under higher tension or have a higher pore formation rate than vesicles without dye. There are several possible mechanisms which could be responsible for this: a) interactions between inclusions; b) stretching of the lipid bilayer by inclusions [21]; or c) the dye molecules enhance the pore formation rate $\nu = \nu_0 \exp[-F_p/k_BT]$ (where F_p is the free energy of a pore, see below). Here, the TR-lipids act as nucleation centers or they reduce the line tension of the lipid bilayer [22] and thus increase the Boltzmann factor $\exp[-F_p/k_BT]$ [23]. In this case, tension stays constant but the pore formation rate ν will depend on ρ, *i.e.* $\nu = \nu(\rho)$.

Here, we do not speculate about the microscopic details leading to enhanced pore formation [24] but rather consider all 3 scenarios. In the following discussion inclusions are taken into account by considering ρ-dependent pore formation rates ν and tensions σ, *i.e.* $\nu = \nu(\rho)$ and $\sigma = \sigma_{in} + \sigma_{el}$, where $\sigma_{in} = \sigma_{in}(\rho)$ is the contribution of the TR-labeled lipids. Cases a)-c) can then be analyzed together by setting $\sigma_{in} \neq 0$ and $\nu = \mathrm{const}$ for case a) and b), and $\sigma_{in} = 0$ and $\nu = \nu(\rho)$ for case c).

The free energy of a pore of radius r in a membrane under tension σ and with line tension λ is given by $F_p = 2\pi r\lambda - \pi r^2\sigma$. For pores with critical radius $r^* = \lambda/\sigma$ this activation barrier is the largest with $F_p(r^*) = \pi\lambda^2/\sigma$. Here, we analyze the dynamics of pore formation of adhering vesicles which are under tension $\sigma = \sigma_{in} + \sigma_{el}$.

Pores are formed by nucleation events. A pore is not stable and its time-dependent radius $r = r(t)$ obeys $2\eta_m \mathrm{d}r/\mathrm{d}t = r\sigma - \lambda$, where η_m is the membrane viscosity [25]. As the pore opens the tension in the membrane decreases. Therefore, $\sigma = \sigma(r)$ in the last equation. It is useful to introduce the lipid area of the bilayer A_0 for which $\sigma(A_0) = 0$. The associated pore size r_c (where $A_i = A_0 + \pi r_c^2$) is given by $\pi r_c^2 = A_i\sigma_i/k_a$. For $\sigma_{in} = 0$ one has $r \leq r_c$.

While the pore is open the volume of the vesicle decreases $-\mathrm{d}V(\theta,R)/\mathrm{d}t = -\Delta P r^3/3\eta$, where the pressure difference driving the volume loss is given by $\Delta P = -2(\sigma_{in}+\sigma_{el})/R$ [26]. In the following, we assume that the shape of a vesicle with pore can also be parameterized by a spherical cap of radius $R(t)$ and contact angle $\theta(t)$, where $R(0) = R_i$ and $\theta(0) = \theta_i$, see also fig. 1B. Then, the relative volume loss is given by

$$\delta v \equiv \frac{V(t_c) - V_i}{V_i} = -\frac{3}{2}\frac{\sigma_i}{k_a}\Delta(t_c)\frac{g(\theta_i)}{f(\theta_i)} + \mathcal{O}\left(\frac{\sigma_i^2}{k_a^2}\right), \tag{2}$$

where t_c is the lifetime of the pore and $\Delta \equiv \pi[R_i^2 g(\theta_i) - R^2 g(\theta)]/(A_i - A_0)$. In deriving eq. (2) it has been assumed that the contact area $R^2(t)\sin\theta(t)$ remains constant while the

pore is open. Upon introducing the dimensionless variables, $\hat{t} = t/\tau$, $\hat{r} = r/r_c$, $\hat{\sigma} = \sigma/\sigma_i$, and $\hat{\lambda} = \lambda/\sigma_i r_c$ [with $\tau = 2\eta_m/\sigma_i$ and $\sigma_i = \sigma_{el}(A_i) + \sigma_{in}(A_i)$] the dynamics of pore formation is described by the set of equations

$$\frac{\mathrm{d}\hat{r}}{\mathrm{d}\hat{t}} = \hat{r}\hat{\sigma} - \hat{\lambda}, \qquad \frac{\mathrm{d}\Delta}{\mathrm{d}\hat{t}} = \frac{\hat{\sigma}\hat{r}^3(t)}{r_L} + \mathcal{O}\left(\frac{\sigma_i^2}{k_a^2}\right), \tag{3}$$

$$\hat{\sigma}(t) \;=\; 1 - \hat{r}^2 - \Delta(t). \tag{4}$$

Here, $r_L = 3\pi\eta R_i^2/(8\eta_m r_c)$ is the leakage parameter introduced in [25]. These equations have to be solved for the boundary conditions $r(0) = r_0$ and $\Delta = 0$ (no leakage occurs during the pore formation event). The behavior of the solutions depends strongly on the size of the vesicles since $\hat{\lambda} \sim r^*/r_c \sim r^*/R_i$. Thus, for small vesicles the line tension is dominant in eq. (3) while for large vesicles it is only for large times $t \simeq t_c$.

Regime 1 (small vesicles): $\hat{\lambda} \gg 1$. Here, $\hat{r}(\hat{t}) = \hat{r}_0\left(1 - \hat{t}/\hat{t}_c\right) + \mathcal{O}(\hat{t}^2/\hat{t}_c^2)$, where $\hat{t}_c = \hat{r}_0/\hat{\lambda} + \mathcal{O}(\hat{\lambda}^{-2})$. In this limit $\Delta \ll 1$ and in good approximation $\hat{\sigma} = 1 - \hat{r}^2(\hat{t})$ and $\Delta(\hat{t}) = \int_0^{\hat{t}} \mathrm{d}t \left[\hat{r}^3(t) - \hat{r}^5(t)\right]/r_L$. The last two equations lead to $\Delta(\hat{t}_c) = (3\hat{r}_0^4 - 2\hat{r}_0^6)/(12 r_L\hat{\lambda})$. The mean volume loss is then given by

$$\overline{\delta v} = -\frac{3}{2}\nu_0\frac{\sigma_i}{k_a}\frac{g(\theta_i)}{f(\theta_i)}\int_0^1 \mathrm{d}\hat{r}\Delta(\hat{r})e^{-F_p(\hat{r})/k_BT}, \tag{5}$$

where one can set $\theta = \theta_i$. Furthermore, ν_0 is of the order $\nu_0 \simeq 10^6 - 10^{11}\mathrm{s}^{-1}$ [27]. Generally, $\nu_0 = \nu_0(\sigma_i)$. Kramer's rule implies $\nu_0 = \sigma_i/\zeta$, where the drag coefficient is of the order $\zeta = 8\pi^2\eta R_i/(0.84 + \log 2\pi R_i/h_b)$, where h_b is the bilayer thickness. Since $\hat{\lambda} \gg \hat{\sigma}_i\hat{r}$ only the prefactor (and not the exponential) of the pore formation rate depends on σ_i. Consequently, the rate of volume loss is dominated by pores of size $r \simeq r_\lambda \equiv k_BT/2\pi\lambda$, thus

$$|\overline{\delta v}| = 24\nu_0\frac{\sigma_i^2\eta_m g(\theta_i)}{\pi k_a\lambda\eta f(\theta_i)}\frac{r_\lambda^5}{R_i^2 r_c^3} \sim \frac{r_\lambda^5}{R_i^5}, \tag{6}$$

i.e. the relative volume loss is larger for smaller vesicles. Compared with vesicles without TR-lipids, the enhanced volume loss is either due to an increased $\sigma_i = \sigma_i(\rho)$ (above cases a) and b)), an increased $\nu_0 = \nu_0(\rho)$ or a decreased $\lambda = \lambda(\rho)$ (case c)).

Regime 2 (large vesicles): $\hat{\lambda} \ll 1$. Additionally (for sufficiently large vesicles) $r_L \gg 1$. Pores with $r < r^*$ behave similar to the ones of regime 1. For $r > r^*$, one has to distinguish 3 dynamic regimes. I) The pore (with initial radius r_0) expands for a short time $t_m \ll t_c$ until it reaches its maximum size $r_m = 1 - \hat{\lambda}/2 - 3\hat{\lambda}^2/8 + \mathcal{O}(\hat{\lambda}^3, \hat{\lambda}/r_L)$. II) For $t_m < t < t'$, one has in very good approximation $\hat{r}\hat{\sigma} = c = \text{const}$, leading to $\hat{r}(\hat{t}) = \hat{r}_m - s\hat{t}$, where $s = \hat{\lambda} - c = \hat{\lambda}/(2r_L) + \mathcal{O}(\hat{\lambda}^2, r_L^{-2})$ and thus $\Delta(\hat{t}) = \hat{\lambda}\left(1 + 2\hat{t}\right)/(2r_L) + \mathcal{O}(\hat{\lambda}/r_L^2)$. III) For $t > t'$, the pore radius $\hat{r}$ becomes small and $\hat{r}(\hat{t}) = \hat{r}(\hat{t}') - \hat{\lambda}\hat{t}$. In leading order $\Delta(\hat{t}_c)$ (where $\hat{t}_c \sim r_L/\hat{\lambda}$) is independent of R_i since $\hat{r}_m$ is independent of $\hat{r}_0$ and thus $\overline{\delta v} \sim \nu_0(\sigma_i)\sigma_i/k_a$.

Thus, the volume loss associated with pore formation is different for large and small vesicles: while $V(t_c) - V_i \sim R_i^{-2}$ in regime 1 one has $V(t_c) - V_i \sim R_i^3$ in regime 2. The crossover takes place at bulk radii $R_b \simeq R_b^*$, where $R_b^* = \lambda k_a^{1/2}/(2\sigma_i^{3/2})$. With these findings the experimental observations made in ref. [13] can be explained. The loss of the encapsulated dye signal is due to leakage associated with pore formation and occurs when the number of enclosed dye-molecules falls below a critical threshold, *i.e.* $V(t) - V_i \leq V_c$. On the time scale of typical experiments only the small vesicles show a significant loss of inner dye ("pre-rupture"). This is because the probability $p(\delta v)$ of forming a pore which leads to a volume loss

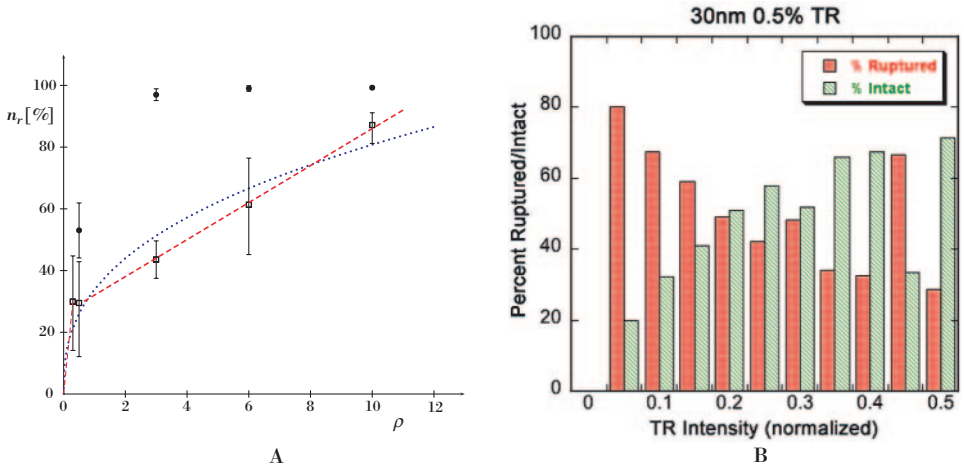

Fig. 2 – (Colour on-line) (A) Percentage of ruptured vesicles (with bulk radius $R = 15\,\text{nm}$ (filled circles) and $R = 25\,\text{nm}$ (squares)) as a function of TR-concentration ρ. The dotted (blue) curve corresponds to the fit $n_r = c\rho^\alpha$ (where $c = 35$, $\alpha = 0.38$, $\chi^2 = 0.68$). The dashed (red) curve is a fit for a bimodal distribution of vesicle sizes and $\sigma \sim \rho$. (B) Histogram of intact and ruptured vesicles (with bulk diameter $2R = 30\,\text{nm}$, 0.5% TR) as a function of their size as measured by their intensity.

of δv is much larger for smaller vesicles than for larger ones. In this way, smaller vesicles are better pore formers and thus appear to be more fusogenic. To test this interpretation we have performed additional experiments in which the dependence of n_r (the fraction of pre-ruptured vesicles) was measured as function of ρ.

Experimental section. – Uni-lamellar vesicles with encapsulated, water soluble dye (carboxy fluorescein, CF) were prepared according to the protocol described in ref. [13] with varying amounts of TR (0.5%, 3%, 6%, and 10%). Vesicles were adhered to a clean glass coverslip at a dilution that allowed visualization of isolated vesicles (1000–10000 fold dilution). The number N_r of pre-ruptured vesicles was measured as a function of the TR-concentration by using a two-color fluorescence setup similar to that of [13] (Nikon TE300 epifluorescence microscope with a 100× oil immersion objective). Vesicles were identified in the TR channel and then the fraction n_{in} of intact TR vesicles showing a colocalized CF signal was determined. The fraction of pre-ruptured vesicles is then $n_r = 1 - n_{in}$ [28]. As shown in fig. 2A, n_r increases with increasing TR-concentration in agreement with our interpretation that larger ρ enhances pore formation. The experimental observation also shows a clear trend that smaller vesicles rupture more often. We can determine the number of intact/ruptured vesicles as a function of their size by taking their TR-intensity as measure for R. As shown in fig. 2B, it is experimentally found that smaller vesicles rupture more often.

To interpret the data presented in fig. 2A we calculate the number of ruptured vesicles from $\overline{\delta v}$. For simplicity, it is assumed that the distribution $p_R(R_b)$ of bulk radii R_b is constant, *i.e.* $p_R(R_b) = (R_{max} - R_{min})^{-1}$ for $R_{min} \leq R_b \leq R_{max}$ and $p_R(R_b) = 0$ otherwise. The vesicles belong to regime 1 since for small ρ a significant fraction of vesicles stays intact (see fig. 2) [29]. Then, for cases a) and b)

$$n_r(\rho) = \int_{R_{min}}^{R_c(\rho)} p_R(R_b)\mathrm{d}R_b = \frac{\sigma_i - \sigma_{min}}{\sigma_{max} - \sigma_{min}}\vartheta(\sigma_i - \sigma_{min})\vartheta(\sigma_{max} - \sigma_i), \tag{7}$$

where $R_c \sim (\sigma_i^2(\rho)/V_c)^{1/2}$, $R_c(\sigma_{min}) = R_{min}$, $R_c(\sigma_{max}) = R_{max}$ and $\vartheta(x)$ is Heaviside's theta function. For large ρ, $\sigma \sim \sigma_i \sim \rho^\alpha$, where, *e.g.*, $\alpha = 2$ for inclusions which interact electrostatically and $\alpha = 1$ for inclusion-induced stretching. Similarly, for case c)

$$n_r(\rho) \sim \left(\frac{\nu_0^{1/2}(\rho)}{\lambda^3} - \frac{\nu_0^{1/2}(\rho_{min})}{\lambda_{min}^3} \right) \Big/ \left(\frac{\nu_0^{1/2}(\rho_{max})}{\lambda_{max}^3} - \frac{\nu_0^{1/2}(\rho_{min})}{\lambda_{min}^3} \right), \tag{8}$$

where $\lambda_{min} = \lambda(\rho_{min})$, $\lambda_{max} = \lambda(\rho_{max})$, $n_r(\rho_{min}) = 0$ and $n_r(\rho_{max}) = 1$. Here, $\lambda \sim \rho^{-\beta}$ or $\nu_0 \sim \rho^\gamma$. Upon fitting the experimental data to the above scaling function (with $\sigma_{min} \simeq 0$) $n_r = n_r(\rho)$ one finds $\alpha \simeq 0.38$ for cases a) and b) and $\beta = 0.13$ and $\gamma = 0.76$ for case c). The large deviation of α from the expected values ($\alpha = 1, 2$) in cases a) and b) probably indicates that the distribution of vesicles is not constant since α depends crucially on $p_R(R_b)$, as can be seen from eq. (7). To illustrate this point we have used a bimodal distribution $p_R(R_b)$ to fit the data for $\alpha = 1$ [30]. The experimental data is also compatible with this distribution showing that for a more quantitative analysis the function $p_R(R_b)$ needs to be known.

The discussed effects are more pronounced for vesicles with inclusions which enhance pore formation. However, our analysis of the pore formation dynamics has also serious consequences for adhering vesicles without additional components. As shown in ref. [11], for adhering vesicles with $R \geq R_{bd}^* \equiv 2\lambda/W$ it is energetically favorable to form a bilayer disk. The transition between these two states is first order. In phase space the two minima (corresponding to an adsorbed vesicle and a bilayer disk) are separated by a local saddle point which can be identified as an adsorbed vesicle with a pore of size $r = r^* = \lambda/\sigma$. Consequently, the transition is driven by pore formation. However, as discussed above, the tension in the membrane is reduced as the pore opens and the size of the pores is limited by σ_i. In particular, for $\sigma_{in} = 0$ all pore radii $r \leq r_c$. Since $r_c \sim R_i$, small vesicles can only form pores with $r < r^*$. More explicitly, pores of radius r^* can only be formed by vesicles with $R \geq R_{cp}^*$ where $r_c(R = R_{cp}^*) = r^*$, and

$$R_{cp}^* = (\lambda k_a^{1/2})/(\sigma_i^{3/2} g^{1/2}(\theta)). \tag{9}$$

Since $R_{cp}^* \geq R_b^*$ only vesicles in volume regime 2 with $R \geq \max\{R_{cp}^*, R_{bd}^*\}$ rupture. For the parameter values used above [29] (and $W \simeq 1.5 \cdot 10^{-4}\,\mathrm{J/m^2}$) one has $R_{cp}^* = 2\,\mu\mathrm{m}$ while $R_{bd}^* = 120\,\mathrm{nm}$. This might explain why in [15] no bilayer disks were seen for vesicles with radii $R \simeq 100\,\mathrm{nm}$. On mica ($W \simeq 5 \cdot 10^{-4}\,\mathrm{J/m^2}$) vesicles of the same size form bilayer disks, which is in agreement with the theoretical predictions, since here $R_{cp}^* = 300\,\mathrm{nm}$ and $R_{bd}^* = 40\,\mathrm{nm}$.

In summary, we have shown theoretically that inclusion-induced tension enhances pore formation and induces leakage in adhering vesicles. The experiments qualitatively confirm the predicted dependency on vesicle size. From a more general point of view, our experiments illustrate that tagging with fluorescent dyes can have a significant influence on the system. The observed destabilization of nanometer-sized vesicles should be relevant for many different experimental situations. It remains a challenge for future work to obtain a more quantitative comparison between theory and experiment. This is a difficult task since the discussed effects are most pronounced for vesicles smaller than the diffraction limit of optical microscopes.

* * *

This work was supported in part by grants from the DAAD, the Fonds der Chemischen Industrie, the NSF Biophysics Program, NIH GM069630, and by the MRSEC Program of the NSF under Award DMR-0213618 (CPIMA).

REFERENCES

[1] Sackmann E., *Science*, **271** (1996) 43.
[2] Brian A. A. and McConnell H. M., *Proc. Natl. Acad. Sci. U.S.A.*, **81** (1984) 6159.
[3] Fix M. *et al.*, *Proc. Natl. Acad. Sci. U.S.A.*, **101** (2004) 7311.
[4] Cornell B. A. *et al.*, *Nature*, **387** (1997) 580.
[5] Song X., Nolan J. and Swanson B. I., *J. Am. Chem. Soc.*, **120** (1998) 4873.
[6] Baksh M. M., Jaros M. and Groves J. T., *Nature*, **427** (2004) 139.
[7] Kalb E., Frey S. and Tamm L. K., *Biochim. Biophys. Acta*, **1103** (1992) 307.
[8] Nissen J. *et al.*, *Europ. Phys. J. B*, **10** (1999) 335.
[9] Watts T. H. *et al.*, *Proc. Natl. Acad. Sci. U.S.A.*, **81** (1984) 7564.
[10] Seifert U. and Lipowsky R., *Phys. Rev. A*, **42** (1990) 4768.
[11] Lipowsky R. and Seifert U., *Mol. Cryst. Liq. Cryst.*, **202** (1991) 17.
[12] Reviakine I. and Brisson A., *Langmuir*, **16** (2000) 1806.
[13] Johnson J. M. *et al.*, *Biophys. J.*, **83** (2002) 3371.
[14] Keller C. A. and Kasemo B., *Biophys. J.*, **75** (1998) 1397.
[15] Schönherr H. *et al.*, *Langmuir*, **20** (2004) 11600.
[16] Lenz P., Ajo-Franklin C. M. and Boxer S. G., *Langmuir*, **20** (2004) 11092.
[17] As shown below the life time of a pore $t_c \simeq 2\eta_m r/\lambda$. The relaxation by diffusive motion of the N inclusions takes place on time scales $t_{rel} \simeq \pi r^2/(4DN)$. For typical parameter values (pore radius $r \simeq 10\,\mathrm{nm}$, line tension $\lambda = 10\,\mathrm{pN}$, membrane viscosity $\eta_m \simeq 5 \cdot 10^{-9}\,\mathrm{Ns/m}$, diffusion coefficient $D \simeq 10\,\mu\mathrm{m}^2/\mathrm{s}$) one has $t_c/t_{rel} \simeq N$, where $N \simeq 100$–1000 in our experiments.
[18] Tordeux C., Fournier J. B. and Galatola P., *Phys. Rev. E*, **65** (2002) 041912.
[19] Fournier J. B., Ajdari A. and Peliti L., *Phys. Rev. Lett.*, **86** (2001) 4970.
[20] Evans E. and Rawicz W., *Phys. Rev. Lett.*, **64** (1990) 2094.
[21] Huang H. W., Chen F. Y. and Lee M. T., *Phys. Rev. Lett.*, **92** (2004) 198304.
[22] Israelachvili J. N. and Marcelja S., *Q. Rev. Biophys.*, **13** (1980) 121; May S., *Eur. Phys. J. E*, **3** (2000) 37.
[23] Schick M., Katsov K. and Müller M., *Mol. Phys.*, **103** (2005) 3055.
[24] Experimentally, we can rule out that the Coulomb interaction between TR-labeled lipids leads to a significant increase in membrane tension since no dependence of the leakage rate on the salt concentration was observed. Furthermore, in ref. [13] adhering vesicles with 5.5% DOPS (a negatively charged lipid) showed no significant content loss.
[25] Brochard-Wyart F., de Gennes P. G. and Sandre O., *Physica*, **278** (2000) 32.
[26] In the experiments (see below) the inner and outer solution are iso-osmolar, which is achieved by dissolving the appropriate amount of NaCl in the outer solution.
[27] Evans E. *et al.*, *Biophys. J.*, **85** (2003) 2342.
[28] In the experiments n_r did not show any significant dependency on observation time τ. However, only $\tau > 100\,\mathrm{s}$ is experimentally accessible (where adhesion starts at $\tau = 0$).
[29] In regime 2, volume exchange is much more efficient since pores with $r_0 > r^*$ expand to radius r_m and on typical experimental time scales (*i.e.* minutes) all vesicles leak and form bilayer disks. This agrees with the theoretical expectation that vesicles with $R \leq 100\,\mathrm{nm}$ belong to regime 1 since $R_b^* = 1\,\mu\mathrm{m}$ (for $\lambda = 10\,\mathrm{pN}$, $k_a = 5 \cdot 10^{-2}\,\mathrm{N/m}$, $\sigma_i = 10^{-4}\,\mathrm{J/m}^2$).
[30] For the fit in fig. 2, one has $p_R(R_b) = \mathrm{const}$ for $R_{min}^{(1)} \leq R_b \leq R_{max}^{(1)}$ and for $R_{min}^{(2)} \leq R_b \leq R_{max}^{(2)}$, $\rho \sim \sigma_i$, $\rho_{min}^{(1)} = 0$, $\rho_{max}^{(1)} = 0.3$, $\rho_{min}^{(2)} = 0.66$ (where $R_c(\rho_{min}^{(i)}) = R_{min}^{(i)}$). Then, $n_r \sim \rho$ for $\rho \leq \rho_{max}^{(1)}$, $n_r = \mathrm{const}$ for $\rho_{max}^{(1)} \leq \rho \leq \rho_{min}^{(2)}$, and $n_r \sim \rho + \mathrm{const}$ for $\rho_{min}^{(2)} \leq \rho \leq \rho_{max}^{(2)}$.